LETTERS

The cargo-binding domain regulates structure and activity of myosin 5

Kavitha Thirumurugan[1], Takeshi Sakamoto[2], John A. Hammer III[3], James R. Sellers[2] & Peter J. Knight[1]

Myosin 5 is a two-headed motor protein that moves cargoes along actin filaments[1,2]. Its tail ends in paired globular tail domains (GTDs) thought to bind cargo[3]. At nanomolar calcium levels, actin-activated ATPase is low and the molecule is folded. Micromolar calcium concentrations activate ATPase and the molecule unfolds[3–6]. Here we describe the structure of folded myosin and the GTD's role in regulating activity. Electron microscopy shows that the two heads lie either side of the tail, contacting the GTDs at a lobe of the motor domain (~Pro 117–Pro 137) that contains conserved acidic side chains, suggesting ionic interactions between motor domain and GTD. Myosin 5 heavy meromyosin, a constitutively active fragment lacking the GTDs, is inhibited and folded by a dimeric GST–GTD fusion protein. Motility assays reveal that at nanomolar calcium levels heavy meromyosin moves robustly on actin filaments whereas few myosins bind or move. These results combine to show that with no cargo, the GTDs bind in an intramolecular manner to the motor domains, producing an inhibited and compact structure that binds weakly to actin and allows the molecule to recycle towards new cargoes.

Myosin 5 has two heavy chains, each contributing an amino-terminal motor domain, an α-helical lever stabilized by six sequentially bound calmodulin light chains, a coiled-coil region that dimerizes with the other heavy chain to form the tail and finally the GTD[3] (Fig. 1o). The unregulated high activity of myosin 5 heavy meromyosin (HMM) implicates the GTD in downregulation of activity at nanomolar calcium. Our initial images of the inhibited state showed a compact conformation, but identification of substructure was ambiguous[4]. The structures seen by other groups were less compact[5,6]. To understand the mechanism of regulation of cargo transport by myosins requires an understanding of the structure and properties of the inhibited state. Therefore we have studied the structure of folded myosin 5, and the GTD's mechanism of inhibition.

Single-particle image processing[7] of folded myosin 5 molecules negative-stained in ATP at nanomolar calcium levels reveals detailed substructure. Briefly, molecules abstracted from raw images (Supplementary Fig. 1) were aligned together, grouped into classes based on image features, and an average image was calculated for each class. Most features are consistent between the class averages (Fig. 1a–e), and identification of substructure is now straightforward (Fig. 1o). The two heads lie either side of an uninterrupted proximal 17 nm segment of the tail, with the head on the left of the tail more clearly delineated and closer to the tail. Within each head, calmodulin subunits of the lever domain can be seen, and the levers overlap at their junction with the tail. Overlap is more extensive in some classes (Fig. 1e), suggesting that levers are flexible. The tail length was highly variable in extended, rotary-shadowed molecules at high ionic strength[3]. In both raw and averaged negatively stained images of the folded state, we see only ~30% of the total predicted coiled coil[3]. Thus, portions of the coiled coil may be unstable and function as elastic linkers between motor and cargo[8]. Preliminary studies of molecules with no nucleotide or with ADP indicate that their structures are similar to those in ATP (Fig. 1h, i).

The motor domains have structural detail that can be reconciled with image averages of single heads and atomic structures. Visual inspection suffices for these comparisons because we have a single two-dimensional view of the molecule, and the features are distinct. The left head closely resembles a proportion of heads of myosin 5 HMM[9] and single heads (S1) (Fig. 1g) in ATP. It also matches well an atomic model built using the crystal structure of the myosin 5 motor domain in the 'post-rigor' conformation with an ATP analogue in the active site[10] (see Supplementary Methods; Fig. 1l). It does not match the pre-powerstroke conformation of myosin 5 HMM[9] or S1 (Fig. 1f) or a pre-powerstroke[11] atomic model oriented to show the same motor domain features (Fig. 1k), primarily because the motor is differently oriented on the lever. Differences in lever shape between folded molecules and models of heads are expected because folding may exert intramolecular strain and the lever is flexible[9] (see next paragraph and Supplementary Information).

The right head motor domain looks different. Its smaller size, strong stain exclusion and pronounced surrounding stain deposit indicate that it is approximately end-on. Its triangular shape is well matched by atomic models with the motor domain almost end-on (Fig. 1m, n). Although the appearance of the right lever resembles the pre-powerstroke model (Fig. 1n), the emergence point of the lever from the motor more accurately matches the post-rigor model (Fig. 1m). Moreover, right heads of molecules in ADP or nucleotide-free resemble those in ATP (Fig. 1h, i), yet are unlikely to occupy the pre-powerstroke state. This head is therefore probably in the same post-rigor conformation as the left head. Differences between images and the post-rigor model arise from lever flexibility[9] (see also Supplementary Information). Thus neither head appears to be in the pre-powerstroke conformation, despite this being the commonest conformation of heads of unregulated HMM in ATP[9].

The GTDs appear as two globules lying between the motor domains. A smaller lobe of the GTD, which touches the motor domain of the left head close to the lever, can be identified because it is absent from images of the head alone (Fig. 1a–e; compare with Fig. 1g; see also Fig. 1o). The length of each GTD (~7 nm) is similar to that of isolated, crystallized GTD from yeast Myo2 (8.8 nm; ref. 12). The consistent location of the smaller lobe indicates specific binding. Comparison with the atomic model (see Supplementary Information) shows that the GTD-binding site on the motor domain appears restricted to a specific segment, chiefly residues Pro 117–Pro 137 (pink in Fig. 1k–n and Fig. 2), and possibly extending to include His 138–Glu 154 (that is, helix E; ref. 13). The small lobe of

[1]Institute of Molecular and Cellular Biology, and Astbury Centre for Structural Molecular Biology, University of Leeds, Leeds LS2 9JT, UK. [2]Laboratory of Molecular Physiology, NHLBI, National Institutes of Health, Bethesda, Maryland 20892-1762, USA. [3]Laboratory of Cell Biology, NHLBI, National Institutes of Health, Bethesda, Maryland 20892-1762, USA.

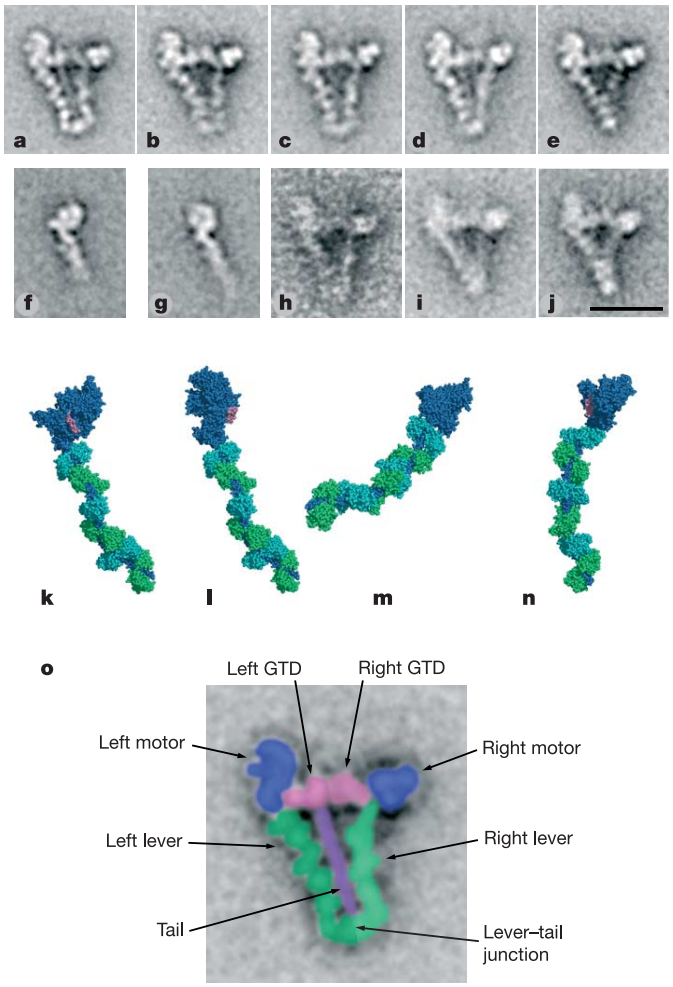

Figure 1 | Structure of switched-off myosin 5 and HMM-GTD complex. **a**–**e**, Averaged images of negative-stained, folded whole myosin molecules; 46–53 molecules per class. **f**, **g**, Averaged images of myosin 5 S1 stained in the presence of ATP; **f** shows the pre-powerstroke conformation (63 molecules), and **g** the post-rigor conformation (58 molecules). **h**, **i**, Averaged images of myosin in the presence of ADP or no nucleotide, respectively; 21 and 55 molecules. **j**, Averaged images of the complex of myosin 5 HMM and GST–GTD dimer; 28 molecules. The scale bar in **j** is 20 nm and applies to panels **a**–**j**. **k**–**n**, Atomic models of myosin 5 head; heavy chain shaded dark blue, the six calmodulins shaded alternately blue and green, and the putative GTD-binding region of the motor domain (Pro 117–Pro 137) shaded pink. **k**, Model using scallop motor domain containing ADP.vanadate[11] oriented to try to match left head of folded myosin in image averages. **l**, Model using myosin 5 motor domain[10] containing ADP.BeF_x oriented to match left head. **m**, Same model as **l**, oriented to match right head. Pro 117–Pro 137 lies behind the converter subdomain in this view. **n**, Same model as **k**, oriented to try to match right head motor domain appearance. Panels **k**–**n** were created using PyMOL (DeLano Scientific). **o**, Enlargement of **a**, coloured and labelled to show domains within folded myosin 5.

GTD associated with the right head is less prominent, but extends into the junction between motor domain and lever, which is the location of Pro 117–Pro 137 in right head models. Within the motor domain, Pro 117–Pro 137 abuts the entrance to the ATP-binding pocket, loop 1 and the β-bulge of the transducer[10], but is far from the actin-binding surface. GTD-induced conformational changes could readily modify nucleotide binding or hydrolysis and, through modifying the properties of the central seven-strand β-sheet, inhibit actin binding and stimulation of ATPase activity (see Supplementary Information). Thus each GTD binds at an equivalent site and acts allosterically, not by physically blocking binding to actin.

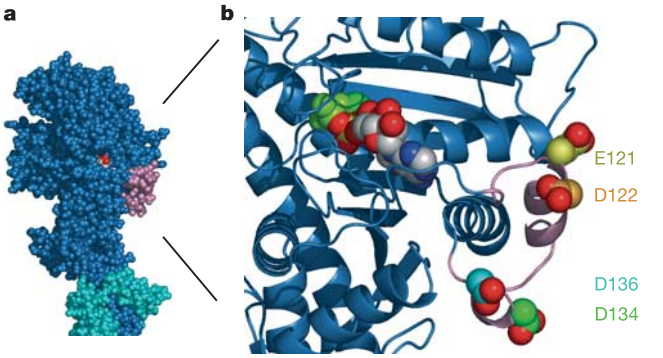

Figure 2 | GTD-binding region of myosin 5 motor domain. **a**, Motor domain region of the myosin 5.ADP.BeF_x complex. The heavy chain is shaded in dark blue, the proximal calmodulin in light blue and the putative GTD-binding region in pink. **b**, Enlargement of the GTD-binding region of the motor domain of **a** to show the spatial relationship to bound nucleotide. The polypeptide chain is shown in cartoon form, except for the four acidic residues (E121, D122, D134, D136) shown in spacefill with their carbon atoms and labels yellow-green, orange, green and light blue respectively and their carboxylate oxygens red. The bound MgADP.BeF_x is shown as a spacefilling model, with ADP shown with carbon silver-grey, oxygen red, nitrogen dark blue and phosphorus yellow, and BeF_x and Mg^{2+} green. The figure was created using PyMOL (DeLano Scientific).

We aligned amino acid sequences at the putative GTD-binding region of the motor domain for myosins 5a, b and c and compared this with other myosin classes (Supplementary Fig. 2). There are 3–4 acidic residues and no basic residues in any myosin 5a or 5b. The carboxy-terminal GDMDP sequence is conserved among vertebrate myosins 5, with conservative substitutions in invertebrates. Other myosin classes have non-conservative substitutions, indicating this may be a site of specificity for myosin 5 regulation. The acidic residues face outwards (Fig. 2b), suggesting ionic interactions with basic residues of the GTD. The densest cluster of basic residues in the GTD is five, within Arg 1800–Lys 1810. This is homologous sequence to helix 13 of the GTD of yeast Myo2, located at the distal end of the GTD[12], and therefore well-suited to match the morphology we see. Ionic interactions are consistent with the salt-sensitivity of folding[4–6].

The role of the GTD in regulation was studied using a glutathione S-transferase (GST)–47 kDa GTD fusion protein. GST is dimeric so the GTD is paired, as in myosin. $(GST–GTD)_2$ inhibits actin-activated MgATPase of myosin 5 HMM at nanomolar calcium levels with an inhibitory dissociation constant K_i of $0.53 \pm 0.14\,\mu M$ (s.d., $n = 5$), but not at micromolar calcium levels (Fig. 3a). GST_2 alone has no effect. Variable residual activity at saturating $(GST–GTD)_2$ partly derives from contaminant single-headed HMM[4]. This is supported by finding that $(GST–GTD)_2$ inhibits S1 more weakly ($K_i = 7.5\,\mu M$; Fig. 3b). The GTD is therefore sufficient to inhibit activity: the intervening sequence between the HMM coiled coil and the GTD is not required. S1 inhibition shows that paired heads are not required for inhibition, but do enhance the effectiveness. Electron microscopy shows that under inhibitory conditions, the HMM–$(GST–GTD)_2$ complex is a compact, triangular shape very similar to folded myosin 5 (Fig. 1j). Similarities include the difference between the shape of the two heads, and the shape and location of the GTDs, consistent with their binding the same sites as in myosin. $(GST)_2$, of mass (51 kDa) similar to a single GTD, is not visible, possibly being obscured by the central pool of stain.

It is a long-standing paradox that at nanomolar calcium levels, where ATPase is inhibited, myosin 5 bound to a coverslip moves actin better than at higher calcium concentration[3], and single-molecule motility assays show individual myosin 5 molecules moving along actin[14–16]. Discovery of the folded conformation at nanomolar calcium levels did not solve this puzzle, because folding echoes the

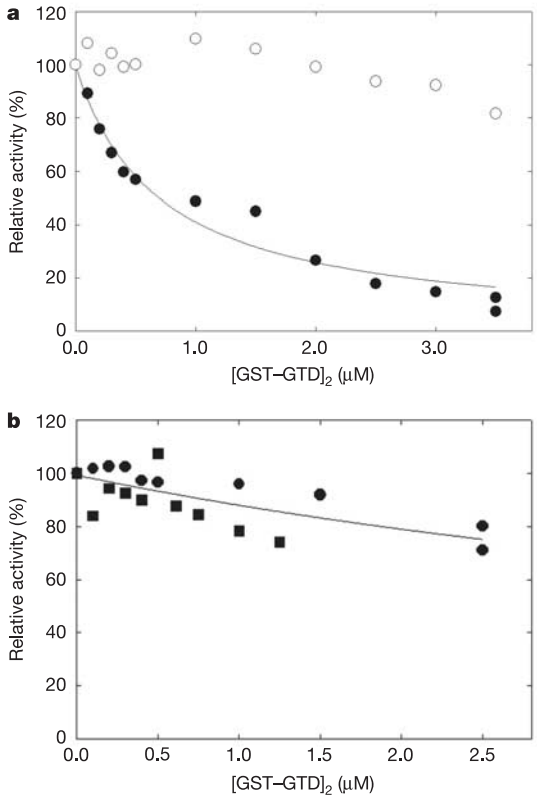

Figure 3 | Regulation of actin-activated myosin 5 ATPase activity by GST-GTD dimers. a, Myosin 5 HMM; solid circles at nanomolar calcium, open circles with 0.1 mM free calcium. The fitted line gives $K_i = 0.75\,\mu M$. **b**, Myosin 5 S1 at nanomolar calcium levels; squares and circles represent independent experiments. Activity is relative to ATPase in the absence of GST–GTD dimers. Ca^{2+} did not greatly affect the Michaelis constant (K_m) values for actin activation of HMM MgATPase which were generally in the range of 0.3–0.7 μM in the presence of 50 mM KCl.

'off'-state of myosin 2 and kinesin[17,18]. We addressed this paradox using two-colour TIRF (total internal reflection fluorescence) microscopy to measure simultaneously the single molecule motility of GFP–HMM and Cy3-myosin in mixtures interacting with the same actin filaments. Observing both species interacting with the same actin filaments overcomes difficulties of comparison between separate experiments. Without ATP, the filaments became heavily decorated with both proteins (Supplementary Fig. 3). With ATP, labelling was lighter with rapid movements of both proteins (see Supplementary Movies). The frequency of movements of each protein showed HMM movements (560 events per 100 pM HMM per min) were much more frequent than myosin movements (14 events per 100 pM myosin per min). This indicates that the great majority of myosin molecules do not move on actin, owing to being switched off. Including 2.5 μM $(GST–GTD)_2$ in the mixtures reduced HMM movements from 660 ± 50 to 317 ± 26 events ± s.d. per 100 pM per min, but myosin movements were unaffected (16 ± 6 to 15 ± 6 events per 100 pM per min), showing that the assay senses inhibition of activity. Myosins that move are probably either a small proportion of molecules that cannot fold or molecules that are unfolded when they collide with actin owing to the folded–unfolded equilibrium. Movement of a small proportion of myosin molecules explains the residual actin activation of myosin 5 ATPase[3,4,6] and the movements seen in earlier studies, and thus largely explains the paradox. *In vitro*, calcium disrupts the folded state and stimulates ATPase activity. Neither motor nor GTD binds calcium, so structural changes linked to calcium binding by calmodulins in the lever are the probable cause. In particular, dissociation of calcium-calmodulin from the lever, weakening it, is implicated in lowering motility[6,19]. This explains why the few active molecules at nanomolar calcium concentrations move actin better. Calcium-induced calmodulin dissociation may also disrupt the geometry required for inhibitory motor domain–GTD interactions, explaining how calcium stimulates ATPase activation by actin.

TIRF shows few, if any, long-lived (>1 s) stationary transient attachments of myosin to actin in ATP at nanomolar calcium concentrations. Moreover, electron microscopy of myosin–actin mixtures under these conditions shows detached, folded myosin and undecorated actin (Supplementary Fig. 4a). In contrast, with no nucleotide or with ADP or ADP + phosphate, TIRF shows heavy decoration, and electron microscopy shows that bundles of myosin-decorated actin filaments are immediately formed in solution (Supplementary Fig. 4b–d). Thus the folded molecules in ATP bind only weakly to actin with a fast 'off' rate, but under other conditions they bind more tightly.

The mechanism of myosin 5 regulation we have described differs from myosin 2, which uses head–head and head–proximal tail interactions[17,20,21] and therefore has regulated HMM[20]. Myosin 5 has more similarities with kinesin, in which a GTD binds the motor domain, slows ADP release and reduces microtubule affinity[18].

The GTD binds cargo receptor proteins as well as the motor domain. Activation of myosin 5 *in vivo* may therefore entail receptor proteins binding to the GTD, weakening the GTD–motor domain interactions we have described and allowing the heads to interact with actin[22]. Our data indicate that the folded molecule binds weakly to actin, so would be able to diffuse freely in cells. After myosin 5 dissociates from cargo at the cell periphery, folding would allow recycling to bind new cargo elsewhere in the cell.

METHODS

Proteins. The GST–GTD fusion protein comprised the C-terminal 414 residues of myosin 5a, encompassing the entire GTD, which was amplified by polymerase chain reaction (PCR) with Ultra High Fidelity Pfu (Stratagene) with *Bam*H1/*Eco*R1 ends, cloned into pGex-4T1 (Amersham) and expressed and purified by standard techniques. Other protein preparations are detailed in Supplementary Methods.

MgATPase assay. Actin-activated MgATPase assays were performed as previously described[23] using 20–40 nM HMM or S1, 10 μM actin, 50 mM KCl, 2 mM $MgCl_2$, 1 mM ATP, 0.1 mM EGTA, 10 mM MOPS (pH 7.0), 40 units per ml lactate dehydrogenase, 1 mM phosphoenolpyruvate, 200 units per ml pyruvate kinase, 200 μM NADH, 2 μM calmodulin at 25 °C. $CaCl_2$, if added, was 0.2 mM.

Single-molecule motility assay. Single-molecule TIRF assays were performed as described previously[23], except that a two-colour observation system (Dual view system, Optical Insights) was used to simultaneously view both GFP–HMM and Cy3-labelled myosin. 6–75 pM GFP–HMM and 60–4,000 pM Cy3-myosin were added into a flow chamber in the presence of ATP and recorded at a frame rate of $2\,s^{-1}$. The number of moving spots on all actin filaments was counted in a $22 \times 44\,\mu m^2$ area on both channels. Further detail is given in Supplementary Methods.

Electron microscopy and image processing. Typically, 40 nM myosin, 480 nM calmodulin, 100 mM KCl, 1.5 mM $MgCl_2$, 20 μM ATP, 0.1 mM EGTA, 2 mM potassium phosphate, 10 mM MOPS, pH 7.0 at 20 °C was applied to a carbon-coated electron microscope grid and immediately stained with uranyl acetate[24]. In some experiments ATP was replaced by hexokinase + glucose treated ADP (1.25 mM) or the same plus potassium phosphate (25 mM), or myosin was treated with apyrase. Actin, when present, was 0.75 μM, pre-treated with hexokinase + glucose or apyrase as needed. HMM–GTD complex comprised 40 nM HMM, 60 nM GST–GTD dimer, 55 μM ATP in the above buffer. Images were processed using SPIDER as described[24]. Further detail is given in Supplementary Methods.

Received 24 March; accepted 3 May 2006.

1. Vale, R. D. Myosin V motor proteins: marching stepwise towards a mechanism. *J. Cell Biol.* **163**, 445–450 (2003).
2. Sellers, J. R. & Veigel, C. Walking with myosin V. *Curr. Opin. Cell Biol.* **18**, 68–73 (2006).
3. Cheney, R. E. *et al.* Brain myosin-V is a 2-headed unconventional myosin with motor-activity. *Cell* **75**, 13–23 (1993).
4. Wang, F. *et al.* Regulated conformation of myosin V. *J. Biol. Chem.* **279**, 2333–2336 (2004).

5. Li, X. D., Mabuchi, K., Ikebe, R. & Ikebe, M. Ca^{2+}-induced activation of ATPase activity of myosin Va is accompanied with a large conformational change. *Biochem. Biophys. Res. Commun.* **315,** 538–545 (2004).
6. Krementsov, D. N., Krementsova, E. B. & Trybus, K. M. Myosin V: regulation by calcium, calmodulin, and the tail domain. *J. Cell Biol.* **164,** 877–886 (2004).
7. Frank, J. *et al.* SPIDER and WEB: Processing and visualization of images in 3D electron microscopy and related fields. *J. Struct. Biol.* **116,** 190–199 (1996).
8. Schilstra, M. J. & Martin, S. R. An elastically tethered viscous load imposes a regular gait on the motion of myosin-V. Simulation of the effect of transient force relaxation on a stochastic process. *J. R. Soc. Interf.* **3,** 153–165 (2006).
9. Burgess, S. *et al.* The prepower stroke conformation of myosin V. *J. Cell Biol.* **159,** 983–991 (2002).
10. Coureux, P. D., Sweeney, H. L. & Houdusse, A. Three myosin V structures delineate essential features of chemo-mechanical transduction. *EMBO J.* **23,** 4527–4537 (2004).
11. Houdusse, A., Szent-Györgyi, A. G. & Cohen, C. Three conformational states of scallop myosin S1. *Proc. Natl Acad. Sci. USA* **97,** 11238–11243 (2000).
12. Pashkova, N., Jin, Y., Ramaswamy, S. & Weisman, L. S. Structural basis for myosin V discrimination between distinct cargoes. *EMBO J.* **25,** 693–700 (2006).
13. Cope, M., Whisstock, J., Rayment, I. & Kendrick Jones, J. Conservation within the myosin motor domain: Implications for structure and function. *Structure* **4,** 969–987 (1996).
14. Sakamoto, T., Amitani, I., Yokota, E. & Ando, T. Direct observation of processive movement by individual myosin V molecules. *Biochem. Biophys. Res. Commun.* **272,** 586–590 (2000).
15. Yildiz, A. *et al.* Myosin V walks hand-over-hand: Single fluorophore imaging with 1.5-nm localization. *Science* **300,** 2061–2065 (2003).
16. Forkey, J. N., Quinlan, M. E., Shaw, M. A., Corrie, J. E. T. & Goldman, Y. E. Three-dimensional structural dynamics of myosin V by single-molecule fluorescence polarization. *Nature* **422,** 399–404 (2003).
17. Wendt, T., Taylor, D., Trybus, K. M. & Taylor, K. Three-dimensional image reconstruction of dephosphorylated smooth muscle heavy meromyosin reveals asymmetry in the interaction between myosin heads and placement of subfragment 2. *Proc. Natl Acad. Sci. USA* **98,** 4361–4366 (2001).
18. Hackney, D. D. & Stock, M. F. Kinesin's IAK tail domain inhibits initial microtubule-stimulated ADP release. *Nature Cell Biol.* **2,** 257–260 (2000).
19. Nguyen, H. & Higuchi, H. Motility of myosin V regulated by the dissociation of single calmodulin. *Nature Struct. Mol. Biol.* **12,** 127–132 (2005).
20. Sellers, J. R. *Myosins* (ed. Sheterline, P.) (Oxford Univ. Press, Oxford, 1999).
21. Ankrett, R. J., Rowe, A. J., Cross, R. A., Kendrick-Jones, J. & Bagshaw, C. R. A folded (10 S) conformer of myosin from a striated muscle and its implications for regulation of ATPase activity. *J. Mol. Biol.* **217,** 323–335 (1991).
22. Li, X. D., Ikebe, R. & Ikebe, M. Activation of myosin Va function by melanophilin, a specific docking partner of myosin Va. *J. Biol. Chem.* **280,** 17815–17822 (2005).
23. Sakamoto, T. *et al.* Neck length and processivity of myosin V. *J. Biol. Chem.* **278,** 29201–29207 (2003).
24. Burgess, S. A., Walker, M. L., Thirumurugan, K., Trinick, J. & Knight, P. J. Use of negative stain and single-particle image processing to explore dynamic properties of flexible macromolecules. *J. Struct. Biol.* **147,** 247–258 (2004).

Supplementary Information is linked to the online version of the paper at www.nature.com/nature.

Acknowledgements We thank S. A. Burgess for expert advice and assistance with image processing, F. Zhang for technical assistance and The Wellcome Trust for support. T.S. was supported by a fellowship from the Japanese Society for the Promotion of Science.

Author contributions Electron microscopy and image processing were performed by K.T., TIRF microscopy by T.S., ATPase assays by J.R.S., and protein preparations by T.S. GST–GTD was created by J.A.H., molecular models by P.J.K., sequence alignments by J.R.S. and P.J.K., and the paper by all authors. J.R.S. and P.J.K. contributed equally to this work.

Author Information Reprints and permissions information is available at npg.nature.com/reprintsandpermissions. The authors declare no competing financial interests. Correspondence and requests for materials should be addressed to P.J.K. (p.j.knight@leeds.ac.uk).